LETTER

doi:10.1038/nature11448

Crystal structure of the multidrug transporter P-glycoprotein from *Caenorhabditis elegans*

Mi Sun Jin[1], Michael L. Oldham[2], Qiuju Zhang[2] & Jue Chen[1,2]

P-glycoprotein (P-gp) is an ATP-binding cassette transporter that confers multidrug resistance in cancer cells[1,2]. It also affects the absorption, distribution and clearance of cancer-unrelated drugs and xenobiotics. For these reasons, the structure and function of P-gp have been studied extensively for decades[3]. Here we present biochemical characterization of P-gp from *Caenorhabditis elegans* and its crystal structure at a resolution of 3.4 ångströms. We find that the apparent affinities of P-gp for anticancer drugs actinomycin D and paclitaxel are approximately 4,000 and 100 times higher, respectively, in the membrane bilayer than in detergent. This affinity enhancement highlights the importance of membrane partitioning when a drug accesses the transporter in the membrane[4]. Furthermore, the transporter in the crystal structure opens its drug pathway at the level of the membrane's inner leaflet. In the helices flanking the opening to the membrane, we observe extended loops that may mediate drug binding, function as hinges to gate the pathway or both. We also find that the interface between the transmembrane and nucleotide-binding domains, which couples ATP hydrolysis to transport, contains a ball-and-socket joint and salt bridges similar to the ATP-binding cassette importers[5], suggesting that ATP-binding cassette exporters and importers may use similar mechanisms to achieve alternating access for transport. Finally, a model of human P-gp derived from the structure of *C. elegans* P-gp not only is compatible with decades of biochemical analysis[6–12], but also helps to explain perplexing functional data regarding the Phe335Ala mutant[13,14]. These results increase our understanding of the structure and function of this important molecule.

P-glycoprotein uses the energy from ATP hydrolysis to pump substrates across the cell membrane. Drug transport depends on ATP hydrolysis[15,16], and the ATPase activity of P-gp is stimulated by the transported drugs[17–19]. *Caenorhabditis elegans* P-gp is 46% identical to human P-gp. To ensure that this level of sequence identity translates into functional similarity, we tested whether overexpression of *C. elegans* P-gp confers cellular resistance to cytotoxic drugs known to be transported by human P-gp. Two potent anticancer drugs, actinomycin D and paclitaxel (Taxol) kill *Spodoptera frugiperda* (Sf9) cells at concentrations greater than 0.1 μM (Fig. 1a). In comparison, cells infected by recombinant baculoviruses carrying the *C. elegans* P-gp gene are resistant to these drugs in concentrations more than 1,000-fold higher (Fig. 1a and Supplementary Fig. 1a). Using detergent-purified protein, we measured whether substrates of human P-gp also stimulate the ATPase activity of *C. elegans* P-gp. Among the 30 compounds we screened, actinomycin D, paclitaxel, progesterone, dipyridamole, and valinomycin increased the ATPase activity of *C. elegans* P-gp more than fivefold (Fig. 1b and Supplementary Fig. 1b). As expected for an ATP-binding cassette (ABC) transporter, both the basal and drug-stimulated levels of ATPase activity are inhibited by vanadate (Fig. 1b). The ATPase activity plotted as a function of drug concentration shows the characteristic biphasic response: with increasing drug concentration, ATPase activity increases to a maximum value and then decreases (Fig. 1c). This behaviour has been studied extensively with human P-gp[20,21]. Like the P-glycoproteins identified in other species[22], the substrate profile of *C. elegans* P-gp only partly overlaps with that of human P-gp. Nevertheless, the similarities between their amino-acid sequences and functional properties suggest that the structure of *C. elegans* P-gp would be a reasonable starting point for a mechanistic understanding of how human P-gp functions as a multidrug pump.

P-glycoprotein is a single polypeptide with two homologous halves, each containing a transmembrane domain (TMD) and a cytoplasmic nucleotide-binding domain (NBD) (Fig. 2a). Crystals of *C. elegans* P-gp were obtained in the absence of nucleotides and transport substrates. The structure was determined at a resolution of 3.4 Å and the amino-acid assignments were confirmed by 34 selenium-labelled methionines and three mercury-labelled cysteines (Supplementary Fig. 2 and Supplementary Table 1).

Compared with the crystal structure of mouse P-gp determined at a resolution of 3.8 Å (ref. 23), that of *C. elegans* P-gp shows a similar

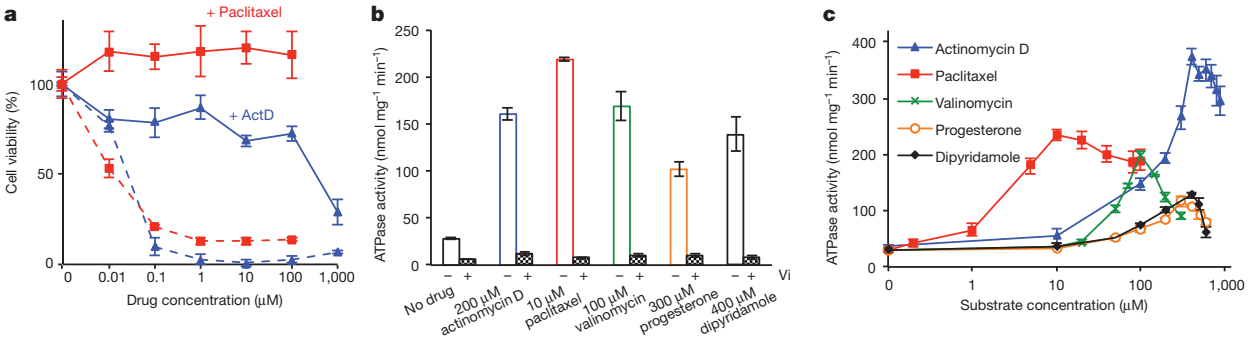

Figure 1 | *Caenorhabditis elegans* P-gp is a multidrug transporter. **a**, Cytotoxicity assay. *Spodoptera frugiperda* Sf9 cells expressing P-gp were cultured with various concentrations of actinomycin D (ActD, blue line) or paclitaxel (red line). Uninfected cells were cultured in the presence of the same drugs as controls (dashed lines). **b**, ATPase activity in the presence and absence of 1 mM orthovanadate. **c**, ATPase activity as a function of substrate concentration. The protein concentration was kept at 0.15 μM for all measurements. Data points represent the means and standard deviations of triplicate measurements from the same preparation.

[1]Department of Biological Sciences, Purdue University, Indiana 47907, USA. [2]Howard Hughes Medical Institute, West Lafayette, Indiana 47907, USA.

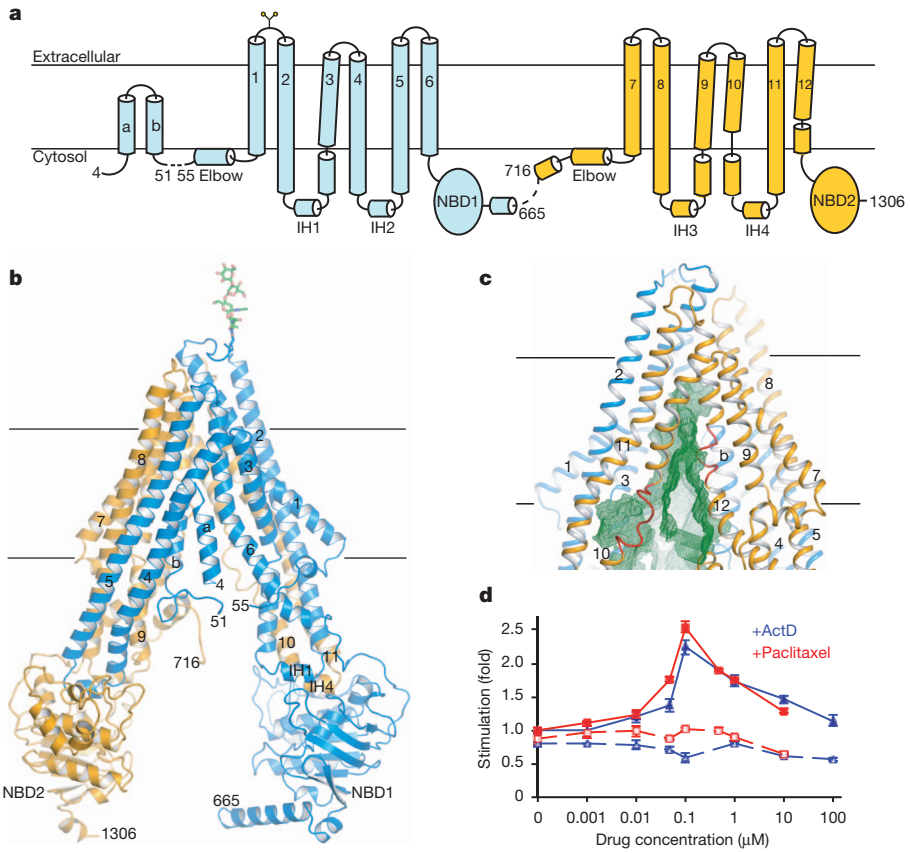

Figure 2 | The molecular architecture of P-gp. **a**, Secondary structure. **b**, Ribbon presentation. **c**, The transmembrane cavity (green mesh) open to the cytosol and continuous with the membrane inner leaflet. The loops in TM10 and TM12 are coloured red. **d**, Drug-stimulated ATPase activities in isolated membranes. The differences measured in the absence and presence of vanadate (1 mM) are plotted. Membranes from untransfected cells were used as controls (dashed lines). The data points show the means and standard deviations of three determinations from the same preparation. These results have been reproduced using different protein preparations.

inward-facing conformation (that is, one open to the cytoplasm), with a larger degree of separation between the two NBDs (Fig. 2b and Supplementary Fig. 3). Superposition of the transmembrane helices individually shows that sequence assignments of six comparable helices (TM1, TM2, TM6, TM7, TM8 and TM11) agree well. The two structures have different conformations in TM9, TM10 and TM12 and these helices thus cannot easily be compared. Helices TM3, TM4 and TM5, which can be compared, show important differences due to register shifts in model building (Supplementary Figs 4–6). As we will discuss later, these corrections in the structure are relevant to the identification of drug-interacting amino acids and an accurate definition of the NBD–TMD interface.

In the crystal structure, the drug transport pathway is open to the cytoplasmic surface and is continuous with the membrane inner leaflet (Fig. 2c). Thus, in principle, drugs could gain access to the transport pathway from the aqueous phase as well as the membrane. It has been proposed that P-gp interacts with drugs from the inner leaflet of the membrane instead of the cytoplasm[4] (the 'hydrophobic vacuum' model). On the basis of this hypothesis, P-gp would be expected to be more sensitive to drug stimulation in membranes than in detergents, because most P-gp substrates are highly concentrated in the membrane, with partition coefficients ranging from 100 to 10,000 (ref. 24). In detergents, 400 μM actinomycin D or 10 μM paclitaxel was required to obtain the maximum ATPase activity of purified P-gp (Fig. 1c). The addition of lipid molecules does not change the apparent drug affinities. Using membranes from yeast cells overexpressing *C. elegans* P-gp, we showed that both drugs stimulate the ATPase activities at a concentration of 0.1 μM (Fig. 2d), which is a 4,000-fold increase in sensitivity for actinomycin D and a 100-fold increase for paclitaxel. The degree of stimulation was lower when using the membrane sample than when using purified P-gp in detergent, probably owing to baseline activity of other cellular ATPases in the yeast cell membranes. We note that the dependence on drug concentration of ATPase stimulation in membranes matches well the concentration dependence observed in the cell protection assay (Figs 1a and 2d). The shift in drug sensitivity in membranes supports the hypothesis that drugs enter the transporter through the membrane's inner leaflet. Such a mechanism, whereby transport depends on an elevated local drug concentration due to membrane partitioning, also implies that the intrinsic affinity of drugs for the transporter itself is low, consistent with the ability of P-gp to transport many different compounds.

The structure of *C. elegans* P-gp presents an interesting variation on the theme of membrane access, in that only one lateral opening is patent (Fig. 2c). An amino-terminal helical hairpin is inserted into the other lateral opening observed in the bacterial exporter MsbA (ref. 25) and mouse P-gp[23] between TM4 and TM6 (Fig. 2b). A truncation mutant devoid of the helical hairpin functions similarly to the full-length protein in a cytotoxic assay (Supplementary Fig. 7a) but has a reduced maximum level of stimulation in an ATPase activity assay (Supplementary Fig. 7b). The dependence on drug concentration, however, is unaltered for the truncation mutant (Supplementary Fig. 7b).

Another notable feature of *C. elegans* P-gp is a discontinuity of helices TM10 and TM12 lining the lateral opening (Fig. 2c). We can think of two possible reasons why the helical secondary structure gives rise to more-disordered loop structures in this region. The first is that a breakdown of secondary structure creates a greater number of possible interactions between protein atoms and drugs entering the pathway. In other transporters where discontinuous transmembrane helices have been observed, the loops inside the membrane have been shown to bind substrates[26]. Thus, loops flanking the lateral opening could assist drug recognition and entry. The second possible reason is that these loop regions could function as flexible hinges to gate the pathway, mediate conformational changes associated with drug transport or both.

The NBD–TMD interface is important in ABC transporters because it transmits conformational changes associated with ATP hydrolysis to substrate translocation. In all ABC importers for which structures have been determined, the TMD is connected to the NBD through a 'ball-and-socket' joint[5]. This joint consists of a cytoplasmic helix from the TMD known as the coupling helix or EAA loop (the ball), which docks into a cleft on the NBD surface (the socket) (Fig. 3a). A similar

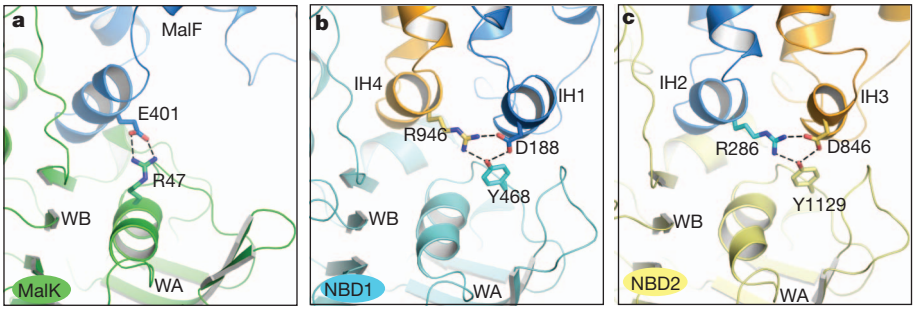

Figure 3 | Interactions between the TMDs and NBDs. **a**, NBD–TMD interface of the maltose importer. MalF is the transmembrane subunit and MalK is the NBD. Glu 401 is the conserved glutamate residue in the EAA loop. **b**, **c**, NBD1–TMD (**b**) and NBD2–TMD (**c**) interfaces in P-gp. Dash lines indicate the conserved salt bridges and hydrogen bonds. WA, Walker A motif; WB, Walker B motif.

structural feature is observed in P-gp, in which intracellular helices IH2 and IH4 on the TMDs resemble the coupling helices and engage the same surface of the NBDs (Fig. 3b, c). In addition to the ball-and-socket joint, ABC exporters, including P-gp, have an additional set of interactions in which IH1 and IH3 also interact with the NBDs, creating a more extensive interaction surface between the TMDs and the NBDs (Fig. 3b, c). The importance of this interface in P-gp to both structure and function is underscored by the high degree of amino-acid conservation, which approaches 80% identity between *C. elegans* and human P-gp (Supplementary Figs 8 and 9).

Multiple crystal structures of the maltose importer show that the transition between different structures is accompanied by rotations of the EAA loop inside the cleft[27]. Salt bridge interactions seem to be central to tethering a pivot point in these conformational changes; elimination of the salt bridges by double mutations results in a defective transporter and dissociation of the MalK subunit[28]. For the NBD1–TMD interface in P-gp, three highly conserved residues, Arg 946 (IH4), Asp 188 (IH1) and Tyr 468 (NBD1), are engaged in a network of salt bridge interactions (Fig. 3b). The same atomic interactions are also observed in the NBD2–TMD interface, involving residues Arg 286 (IH2), Asp 846 (IH3) and Tyr 1129 (NBD2) (Fig. 3c). It is likely that these interactions in P-gp have a role similar to the salt bridge interactions in importers such as the maltose transporter.

To assist structural and functional analysis of human P-gp, we generated a homology model of human P-gp based on the structure of the *C. elegans* P-gp determined in this study. The modelled structure is consistent with a large body of biochemical and biophysical data on human P-gp (Fig. 4 and Supplementary Fig. 10). For example, pairs of residues in the TMDs shown by cysteine mutagenesis to form disulphide bonds[6,7] are located in close proximity to each other (Fig. 4b, c). The NBD–TMD interfaces are consistent with data showing that Ala 266 in TMD1 is in close proximity to Phe 1086 in NBD2[29] and that cysteines introduced at positions 443 and 474 in NBD1 crosslink with residues 909 and 905 in TMD2, respectively[12] (Fig. 4d, e). Residues protected by drug substrates from inhibition by thiol-reactive analogues are suggested to form the drug-binding region[8–11]. In the modelled structure, 17 of the 19 residues are distributed on the surface of the drug-translocation pathway (Fig. 4f). Most of these residues are non-polar, consistent with the hydrophobic nature of the substrates. In contrast, the 17 residues that were not protected by substrate, and therefore are presumed to be not involved in drug binding[11], are scattered throughout the TMDs (Fig. 4f). Previously, the orientations of TM3, TM4 and TM5 with respect to the drug-translocation pathway predicted by arginine-scanning mutagenesis were incompatible with the crystal structure of mouse P-gp[30]. On correction of amino-acid registry (Supplementary Figs 5 and 6), these biochemical data are now consistent with the homology-modelled human P-gp (Supplementary Fig. 10).

The atomic structure of P-gp offers insights into functional data that otherwise are difficult to explain. For example, mutants that enhance

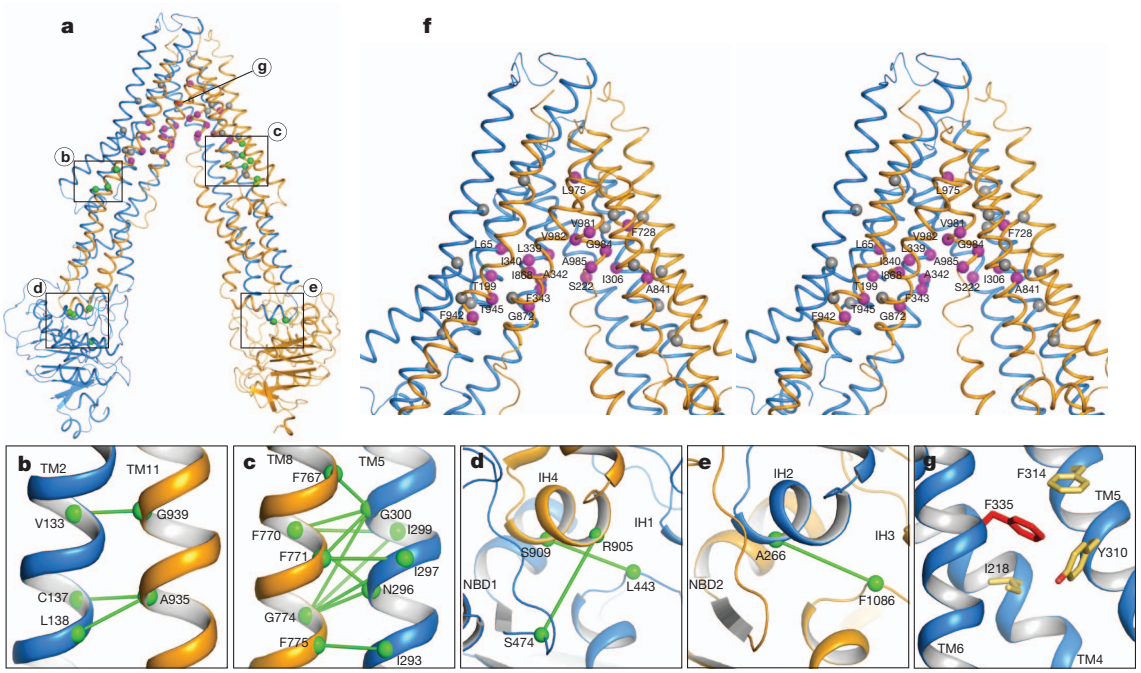

Figure 4 | A model of human P-gp. **a**, Overall structure. **b**, **c**, Pairs of residues in TMDs that formed disulphide bonds (green line) when mutated to cysteines[6,7]. **d**, **e**, Pairs of residues at the NBD–TMD interfaces that were crosslinked[12,29]. **f**, Stereo view of the drug transport pathway. Drug-interacting residues[8–11] are labelled and shown as magenta balls. The non-protected residues, Tyr 118, Val 125, Val 133, Cys 137, Gln 195, Asn 296, Gly 300, Tyr 310, Phe 314, Ala 729, Phe 759, Ser 766, Gly 774, Asn 842, Ala 871, Ser 943 and Phe 957, are shown in grey[11]. **g**, Phe 335 in TM6 (red) interacts with residues in TM4 and TM5 (yellow sticks), thereby stabilizing the inward-facing conformation.

drug-stimulated ATPase activity often show stronger resistance to the same drug, probably owing to an increased affinity for the drug. However, this correlation does not hold for the Phe335Ala mutant, which has a higher ATPase activity but confers lower or similar drug resistance[13,14]. The structure shows that Phe 335 is located at the apex of the drug transport pathway, making van der Waals interactions with Tyr 310 and Phe 314 in TM5, and Ile 218 in TM4 (Fig. 4a, g). These contacts will be broken in the outward-facing conformation, in which the transport pathway has to be continuous with the extracellular side of the membrane[25]. Mutating the phenylalanine to alanine, if doing so destabilized the inward-facing conformation, would facilitate the transition to the outward-facing conformation and thus give rise to higher basal and drug-stimulated ATPase activities. In this description, the Phe335Ala mutant would be reminiscent of mutants identified in the maltose transporter that allow constitutive ATP hydrolysis in the absence of the binding protein[27].

The structure of *C. elegans* P-gp provides an accurate model with which to interpret decades of functional and biochemical data on P-gp. The functional data complement the crystal structure to support a picture in which P-gp uses the energy from ATP hydrolysis to expel lipophilic molecules from the inner leaflet of the membrane. Many details of this molecule, such as how substrate binding activates the ATPase activity, how ATP hydrolysis is coupled to substrate flipping and how multiple substrates are recognized by a single transporter, remain to be elucidated.

METHODS SUMMARY

The gene encoding *C. elegans* P-gp was synthesized and optimized for expression in yeast and insect cells (Bio Basic Inc.). Native protein was expressed in *Pichia pastoris* strain SMD1163 and selenomethionine-substituted protein was expressed in Hi5 cells. The cytotoxicity assays were performed using baculovirus-infected *S. frugiperda* Sf9 cells and the ATP/NADH coupled assays were carried out at 25 °C. Crystals were obtained at 4 °C by the vapour diffusion method. Diffraction data were collected at the Advanced Photon System at Argonne National Laboratory. The initial phase was obtained by molecular replacement (PHASER, CCP4) using separate domains of Sav1866 and mouse P-gp structures as search models. The molecular replacement phase was combined with single-wavelength anomalous dispersion phasing (PHASEREP, CCP4) to identify selenomethionine-substituted residues and mercury-labelled cysteines. The model was built in COOT and refined using CNS and REFMAC5. The human P-gp model was generated using MODELLER (http://salilab.org/modeller/about_modeller.html).

Full Methods and any associated references are available in the online version of the paper.

Received 3 March; accepted 27 July 2012.
Published online 23 September 2012.

1. Juliano, R. L. & Ling, V. A surface glycoprotein modulating drug permeability in Chinese hamster ovary cell mutants. *Biochim. Biophys. Acta* **455,** 152–162 (1976).
2. Ueda, K. *et al.* The mdr1 gene, responsible for multidrug-resistance, codes for P-glycoprotein. *Biochem. Biophys. Res. Commun.* **141,** 956–962 (1986).
3. Sharom, F. J. The P-glycoprotein multidrug transporter. *Essays Biochem.* **50,** 161–178 (2011).
4. Higgins, C. F. & Gottesman, M. M. Is the multidrug transporter a flippase? *Trends Biochem. Sci.* **17,** 18–21 (1992).
5. Oldham, M. L., Davidson, A. L. & Chen, J. Structural insights into ABC transporter mechanism. *Curr. Opin. Struct. Biol.* **18,** 726–733 (2008).
6. Loo, T. W., Bartlett, M. C. & Clarke, D. M. Val133 and Cys137 in transmembrane segment 2 are close to Arg935 and Gly939 in transmembrane segment 11 of human P-glycoprotein. *J. Biol. Chem.* **279,** 18232–18238 (2004).
7. Loo, T. W., Bartlett, M. C. & Clarke, D. M. Disulfide cross-linking analysis shows that transmembrane segments 5 and 8 of human P-glycoprotein are close together on the cytoplasmic side of the membrane. *J. Biol. Chem.* **279,** 7692–7697 (2004).
8. Loo, T. W., Bartlett, M. C. & Clarke, D. M. Transmembrane segment 1 of human P-glycoprotein contributes to the drug-binding pocket. *Biochem. J.* **396,** 537–545 (2006).
9. Loo, T. W., Bartlett, M. C. & Clarke, D. M. Transmembrane segment 7 of human P-glycoprotein forms part of the drug-binding pocket. *Biochem. J.* **399,** 351–359 (2006).
10. Loo, T. W., Bartlett, M. C. & Clarke, D. M. Suppressor mutations in the transmembrane segments of P-glycoprotein promote maturation of processing mutants and disrupt a subset of drug-binding sites. *J. Biol. Chem.* **282,** 32043–32052 (2007).
11. Loo, T. W. & Clarke, D. M. Do drug substrates enter the common drug-binding pocket of P-glycoprotein through "gates"? *Biochem. Biophys. Res. Commun.* **329,** 419–422 (2005).
12. Zolnerciks, J. K., Wooding, C. & Linton, K. J. Evidence for a Sav1866-like architecture for the human multidrug transporter P-glycoprotein. *FASEB J.* **21,** 3937–3948 (2007).
13. Loo, T. W. & Clarke, D. M. Functional consequences of phenylalanine mutations in the predicted transmembrane domain of P-glycoprotein. *J. Biol. Chem.* **268,** 19965–19972 (1993).
14. Loo, T. W. & Clarke, D. M. Rapid purification of human P-glycoprotein mutants expressed transiently in HEK 293 cells by nickel-chelate chromatography and characterization of their drug-stimulated ATPase activities. *J. Biol. Chem.* **270,** 21449–21452 (1995).
15. Azzaria, M., Schurr, E. & Gros, P. Discrete mutations introduced in the predicted nucleotide-binding sites of the mdr1 gene abolish its ability to confer multidrug resistance. *Mol. Cell. Biol.* **9,** 5289–5297 (1989).
16. Hamada, H. & Tsuruo, T. Purification of the 170- to 180-kilodalton membrane glycoprotein associated with multidrug resistance. 170- to 180-kilodalton membrane glycoprotein is an ATPase. *J. Biol. Chem.* **263,** 1454–1458 (1988).
17. Al-Shawi, M. K. & Senior, A. E. Characterization of the adenosine triphosphatase activity of Chinese hamster P-glycoprotein. *J. Biol. Chem.* **268,** 4197–4206 (1993).
18. Ambudkar, S. V. Drug-stimulatable ATPase activity in crude membranes of human MDR1-transfected mammalian cells. *Methods Enzymol.* **292,** 504–514 (1998).
19. Sarkadi, B., Price, E. M., Boucher, R. C., Germann, U. A. & Scarborough, G. A. Expression of the human multidrug resistance cDNA in insect cells generates a high activity drug-stimulated membrane ATPase. *J. Biol. Chem.* **267,** 4854–4858 (1992).
20. Al-Shawi, M. K., Polar, M. K., Omote, H. & Figler, R. A. Transition state analysis of the coupling of drug transport to ATP hydrolysis by P-glycoprotein. *J. Biol. Chem.* **278,** 52629–52640 (2003).
21. Litman, T., Zeuthen, T., Skovsgaard, T. & Stein, W. D. Structure-activity relationships of P-glycoprotein interacting drugs: kinetic characterization of their effects on ATPase activity. *Biochim. Biophys. Acta* **1361,** 159–168 (1997).
22. Ambudkar, S. V., Kim, I.-W. & Booth-Genthe, C. Relationship between drugs and functional activity of various mammalian P-glycoproteins (ABCB1). *Mini Rev. Med. Chem.* **8,** 193–200 (2008).
23. Aller, S. G. *et al.* Structure of P-glycoprotein reveals a molecular basis for poly-specific drug binding. *Science* **323,** 1718–1722 (2009).
24. Gatlik-Landwojtowicz, E., Aanismaa, P. & Seelig, A. Quantification and characterization of P-glycoprotein-substrate interactions. *Biochemistry* **45,** 3020–3032 (2006).
25. Ward, A., Reyes, C. L., Yu, J., Roth, C. B. & Chang, G. Flexibility in the ABC transporter MsbA: alternating access with a twist. *Proc. Natl Acad. Sci. USA* **104,** 19005–19010 (2007).
26. Screpanti, E. & Hunte, C. Discontinuous membrane helices in transport proteins and their correlation with function. *J. Struct. Biol.* **159,** 261–267 (2007).
27. Khare, D., Oldham, M. L., Orelle, C., Davidson, A. L. & Chen, J. Alternating access in maltose transporter mediated by rigid-body rotations. *Mol. Cell* **33,** 528–536 (2009).
28. Mourez, M., Hofnung, M. & Dassa, E. Subunit interactions in ABC transporters: a conserved sequence in hydrophobic membrane proteins of periplasmic permeases defines an important site of interaction with the ATPase subunits. *EMBO J.* **16,** 3066–3077 (1997).
29. Loo, T. W., Bartlett, M. C. & Clarke, D. M. Processing mutations disrupt interactions between the nucleotide binding and transmembrane domains of P-glycoprotein and the cystic fibrosis transmembrane conductance regulator (CFTR). *J. Biol. Chem.* **283,** 28190–28197 (2008).
30. Loo, T. W., Bartlett, M. C. & Clarke, D. M. Identification of residues in the drug translocation pathway of the human multidrug resistance P-glycoprotein by arginine mutagenesis. *J. Biol. Chem.* **284,** 24074–24087 (2009).

Supplementary Information is available in the online version of the paper.

Acknowledgements We thank the beamline staff of the GM/CA CAT at the Advanced Photon System for assistance with data collection, Y.-K. Cho for assistance with protein purification and A. Davidson for comments on the manuscript. We also thank the MacKinnon laboratory for reagents and advice on the *P. pastoris* expression system. This work was supported by Howard Hughes Medical Institute (J.C.), Purdue Center for Cancer Research (NCI CCSG CA23168), and postdoctoral fellowships from the National Research Foundation of Korea and the International Human Frontier Science Program (M.S.J.).

Author Contributions All authors helped design the study and analysed the data. M.S.J. and M.L.O. determined the crystal structure. M.S.J. and Q.Z. performed the biochemical experiments. M.S.J., M.L.O. and J.C. wrote the manuscript.

Author Information Coordinates and structure factors have been deposited in the Protein Data Bank under accession number 4F4C. Reprints and permissions information is available at www.nature.com/reprints. The authors declare no competing financial interests. Readers are welcome to comment on the online version of the paper. Correspondence and requests for materials should be addressed to J.C. (chenjue@purdue.edu).

METHODS

Cloning, expression and purification. A synthetic gene encoding the full-length *C. elegans* P-gp (*pgp-1*; GenBank accession code, AB01232.1) was subcloned into the pPICZ (Invitrogen) and pVL1393 (BD Biosciences) vectors. The carboxy terminus of P-gp was fused to enhanced green fluorescence protein (eGFP) plus a deca-histidine tag or the Protein A tag derived from pEZZ18 (GE Healthcare). A PreScission protease cleavage site was engineered between P-gp and the C-terminal tag.

Native protein was expressed in *P. pastoris* strain SMD1163 (Invitrogen). Cells were grown at 28 °C in minimal methanol medium and induced with 0.5% methanol for 24 h. After collection by centrifugation (4,000*g* for 15 min), the cells were frozen in liquid nitrogen and broken by cryomilling (Retsch model MM400). Broken cells were resuspended in lysis buffer containing 50 mM Tris-HCl, pH 8.0, 150 mM NaCl, 20% glycerol, 5 mM $MgCl_2$, 1 mM PMSF, 1 mM benzamidine, 0.1 mg ml^{-1} trypsin inhibitor, 3 μg ml^{-1} DNase, 1 μg ml^{-1} pepstatin A, leupeptin and aprotinin. Membranes were solubilized by adding 1% (w/v) *n*-dodecyl-β-D-maltopyranoside (DDM, Affymetrix) to the lysis buffer and incubating at 4 °C for 2 h. Insoluble membrane was removed by centrifugation at 80,000*g* for 40 min and supernatant was loaded onto cobalt affinity resin (Clontech). After on-column cleavage by PreScission protease, protein was eluted and reloaded onto a GST column to remove the GST-tagged PreScission protease. Protein was concentrated using an Amicon Ultra (MWCO 50K, Millipore) centrifugal device and further purified by Superdex 200 size-exclusion chromatography (GE Healthcare) in a buffer containing 20 mM MES, pH 6.5, 200 mM NaCl, 10% glycerol, 5 mM DTT and 0.02% (w/v) *n*-undecyl-β-D-thiomaltopyranoside (UDTM, Affymetrix).

Selenomethionine-labelled protein was expressed in Hi5 cells (Invitrogen) adapted to methionine-free medium (Expression Systems). Baculovirus-infected Hi5 cells were cultured for 16–20 h at 28 °C, supplemented with 200 mg^{-1} L-(+)-selenomethione (Fisher Scientific), and then incubated for an additional 48 h. Cells were collected and broken using a high-pressure homogenizer (Emulsiflex-C5, Avestin) in the lysis buffer plus 5 mM DTT. Cell debris was removed by low-speed centrifugation (6,000*g*, 20 min) and membranes were collected by high-speed centrifugation (200,000*g*, 1 h). The membranes were homogenized and solubilized with 1% (w/v) DDM for 2 h. Extracted protein was purified using IgG sepharose affinity resin (GE Healthcare) followed by PreScission cleavage to remove the Protein A tag. The protein sample was further purified using GST affinity resin and gel-filtration chromatography. All purification steps were carried out at 4 °C.

Cytotoxicity assay. Sf9 cells infected with recombinant baculovirus carrying the P-gp + eGFP gene were incubated at 28 °C for 24 h before actinomycin D or paclitaxel (Sigma-Aldrich) was added to the medium. Cells were monitored by counting the cell densities every 6 h for 1 d in the presence of actinomycin D or every 24 h for 3 d in the presence of paclitaxel. The percentage cell viability was calculated by dividing the number of live cells cultured with drug by that of the infected cells cultured without drug. In the presence of actinomycin D, cytotoxic effects were observed after 6 h of drug exposure and reached a maximum at 12 h. Paclitaxel-induced cell death was observed after 24 h of drug exposure and reached a maximum at 48 h. P-glycoprotein expression was monitored by fluorescence microscopy. Each assay was repeated in triplicate.

Preparation of microsomes. Cryomilled yeast cells were resuspended in the lysis buffer and the suspension was centrifuged at 4,000*g* for 15 min to remove the cell debris. The supernatant was ultracentrifuged at 200,000*g* for 1 h and the pellet containing the microsome was stored at −80 °C.

ATP hydrolysis assay. The ATPase activity of *C. elegans* P-gp was analysed using a coupled assay in which the regeneration of hydrolyzed ATP was coupled to the oxidation of NADH[31]. Purified protein was added to the ATPase reaction buffer (50 mM potassium HEPES, pH 8.0, 10 mM $MgCl_2$, 60 μg ml^{-1} pyruvate kinase, 32 μg ml^{-1} lactate dehydrogenase, 4 mM phosphoenolpyruvate, 0.3 mM NADH and 5 mM ATP) at 25 °C in the presence or absence of drug substrates. For vanadate inhibition, the protein samples were mixed with 1 mM vanadate in the presence of ATP-Mg for 10 min at room temperature (22 °C) before measuring the ATPase activity. To determine the drug-stimulated ATPase activity of P-gp in the membrane, microsomes (5 μg) were pre-incubated in the reaction buffer with actinomycin D or paclitaxel for 5 min at room temperature. The fold increase in drug stimulation was calculated by deducing the rate of ATP hydrolysis in the presence of vanadate (1 mM) from that in the absence of vanadate.

Crystallization and data collection. Native crystals were obtained by mixing 1 μl of protein sample (10 mg ml^{-1}) and 1 μl of reservoir solution containing 100 mM HEPES, pH 6.6–7.2, 200 mM sodium malonate and 19–22% PEG2000MME at 4 °C using the sitting-drop vapour diffusion method. Mercury-labelled crystals were prepared by adding 1 mM methyl mercury chloride (II) into crystal-containing drops for 4 h at 4 °C. Crystals of selenomethionine-substituted protein were obtained with 100 mM HEPES, pH 6.6–7.2, 200 mM ammonium phosphate monobasic and 19–22% PEG1500 at 4 °C. All crystals appeared within 2 d and continued to grow to full size in one week. Crystals were dehydrated and cryoprotected by a serial increase in PEG concentration in 5% steps in the reservoir (final 30%) for 48 h followed by 2.5% steps in the drop (final 35%) for 2 h. Crystals were flash-frozen in liquid nitrogen. Diffraction data were collected at the 23-ID beamline at the Advanced Photon System. Diffraction images were indexed, integrated and scaled with the HKL2000 package (HKL Research Inc.).

Structure determination and homology modelling. The structure was determined by molecular replacement (PHASER, CCP4)[32] using separate domains of bacterial Sav1866 and mouse P-gp structures as search models. The molecular replacement phase was combined with single-wavelength anomalous dispersion phasing (PHASEREP, CCP4) to identify methionine and cysteine sites. The model was built by iterative modelling in COOT[33] and refined using CNS[34] and REFMAC5[35]. The crystallographic statistics are summarized in Supplementary Table 1. Residues of the N terminus (1–3, 52–54), the linker region (666–715) and the C terminus (1307–1321) were not visible in the electron density map and were not included in the final structure. No residues lie in the disallowed region of the Ramachandran plot. The homology model of human P-gp was generated by the program MODELLER on the basis of the structure of *C. elegans* P-gp in which the N-terminal region and the linker region were excluded because of low sequence conservation (Supplementary Fig. 9). All figures were generated using the program PyMOL (http://www.pymol.org/).

31. Garrigos, M., Belehradek, J. Jr, Mir, L. M. & Orlowski, S. Absence of cooperativity for MgATP and verapamil effects on the ATPase activity of P-glycoprotein containing membrane vesicles. *Biochem. Biophys. Res. Commun.* **196,** 1034–1041 (1993).
32. McCoy, A. J. *et al.* Phaser crystallographic software. *J. Appl. Crystallogr.* **40,** 658–674 (2007).
33. Emsley, P. & Cowtan, K. Coot: model-building tools for molecular graphics. *Acta Crystallogr. D* **60,** 2126–2132 (2004).
34. Brunger, A. T. Version 1.2 of the crystallography and NMR system. *Nature Protocols* **2,** 2728–2733 (2007).
35. Murshudov, G. N., Vagin, A. A. & Dodson, E. J. Refinement of macromolecular structures by the maximum-likelihood method. *Acta Crystallogr. D* **53,** 240–255 (1997).